ChemComm

Cite this: *Chem. Commun.*, 2011, **47**, 11534–11536

www.rsc.org/chemcomm

COMMUNICATION

An aryl-phosphonate appended macrocyclic platform for lanthanide based bimodal imaging agents†

Matteo P. Placidi,[a] Jörn Engelmann,[b] Louise S. Natrajan,[c] Nikos K. Logothetis[ad] and Goran Angelovski*[a]

Received 21st July 2011, Accepted 19th September 2011
DOI: 10.1039/c1cc14437e

Four ligand systems have been prepared whose characteristics are well suited to the design of bimodal MRI and luminescence probes. The lanthanide complexes display high relaxivities and luminescence quantum yields. These properties are retained at higher magnetic fields and in a range of competitive environments including model extracellular medium and cultured cells.

Lanthanide complexes have received much attention recently due to their unique magnetic and optical properties. Gd^{3+} chelates are used to enhance the contrast observed between tissues in magnetic resonance imaging (MRI), providing images at unlimited depths with a high spatial and temporal resolution. Recent efforts have focused on improving the efficacy or more specifically the longitudinal relaxivity (r_1) of these agents, to increase the sensitivity of this technique with the ultimate aim of cellular imaging. Technological advances in MRI have also increased the demand for agents that function effectively at higher field strengths.[1] In parallel, the luminescence from lanthanide probes can be used to provide detailed information through bioassay measurements[2,3] and high resolution images at the sub-cellular level.[4] By employing time gated techniques, interfering background autofluorescence can be suppressed.

The challenge remains to design a suitable ligand system whose attributes suit both modalities.[5–8] Through this approach, a cocktail of magnetically and optically active complexes with identical biodistributions could be administered, to simultaneously exploit the advantages of both techniques and enable a more accurate interpretation of *in vivo* molecular imaging experiments.[9] However, the design of a ligand system suitable for both of these modalities is far from trivial, because of their conflicting requirements for the inner sphere hydration number (q). MRI agents ideally need a high q to ensure an effective magnetic relaxation, whilst maintaining a high stability. Conversely luminescent complexes require a low value of q to minimise the amount of non-radiative deactivation.

Lanthanide chelates appended with a phosphonate moiety may offer an elegant solution to this problem. Previous Gd^{3+} complexes containing this group have shown a higher than expected relaxivity, despite their low q values. This is attributed to the presence of several water molecules that occupy the second coordination sphere.[10–13] Therefore we sought to design a ligand system whose complexes would exhibit favourable characteristics for both luminescence and MRI. This system consists of a kinetically inert macrocyclic binding site covalently linked to an aromatic phosphonate moiety.

This system was chosen for several reasons. Due to the close proximity of the phosphonate group, it can directly coordinate to the lanthanide ion maintaining a low q and simultaneously act as an antenna unit sensitising the metal centred luminescence. Despite the fact that the complex is octa-coordinate at the lanthanide ion, the interactions with the water molecules in the second sphere will ensure an effective relaxivity. Finally structural variation of the ligand platforms, including length of the alkyl chain and nature of the phenolic *para* substituent will enable fine tuning of the resulting physicochemical properties.

A straightforward synthetic route was developed to obtain $\mathbf{L^{1-4}}$ (Fig. 1). Following the monobenzylation of hydroquinone,[14] the phenol **1** was converted to the phosphate ester **2** by reaction with diethyl phosphite in the presence of triethylamine. A phospho-Fries rearrangement was then induced by the addition of LDA resulting in **3**. According to the desired distance between the macrocycle and the aromatic phosphonate, **3** was reacted with either dibromopropane or dibromobutane to give **4** and **5** respectively.

The ligand precursors **6** and **7** were prepared by *N*-alkylation of the tris-*tert* butyl ester derivative of cyclen (tris-*t*-Bu-DO3A[15]). At this stage two different synthetic routes were envisaged for each precursor. The first involved the removal of the phosphonate ethyl and the *tert*-butyl ester groups using Me_3SiBr and trifluoroacetic acid (TFA) in CH_2Cl_2, respectively. These conditions allowed the retention of the benzyl ether to obtain $\mathbf{L^1}$ and $\mathbf{L^3}$ as the main product, with traces of $\mathbf{L^2}$ and $\mathbf{L^4}$ due to the partial cleavage of the ether. However, in

[a] *Department for Physiology of Cognitive Processes, Max Planck Institute for Biological Cybernetics, Spemannstr. 38, 72076 Tübingen, Germany. E-mail: goran.angelovski@tuebingen.mpg.de; Fax: +49 7071 601 919; Tel: +49 7071 601 916*
[b] *High-Field Magnetic Resonance Center, Max Planck Institute for Biological Cybernetics, Tübingen, Germany*
[c] *School of Chemistry, The University of Manchester, Oxford Road, Manchester, UK*
[d] *Imaging Science and Biomedical Engineering, University of Manchester, Manchester, UK*

† Electronic supplementary information (ESI) available: Full synthetic procedures, NMR and photophysical characterisation. See DOI: 10.1039/c1cc14437e

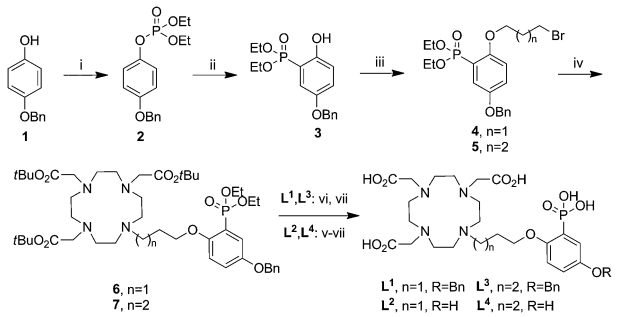

Fig. 1 Synthesis of ligands $\mathbf{L^{1-4}}$: (i) $HP(O)(OEt)_2$, Et_3N, CCl_4; (ii) LDA, THF, −78 °C; (iii) dibromopropane or dibromobutane, K_2CO_3, DMF, 60 °C; (iv) tris-*t*-Bu-DO3A, Cs_2CO_3, CH_3CN, 70 °C; (v) H_2, Pd/C, EtOH, 60 °C; (vi) Me_3SiBr, CH_2Cl_2; (vii) TFA, CH_2Cl_2.

both cases the two ligand systems were readily separated using RP-HPLC. The second route involved the removal of all three protecting groups through catalytic hydrogenation of **6** and **7**, followed by cleavage of the ethyl and *tert*-butyl esters, using the same conditions described above to yield $\mathbf{L^2}$ and $\mathbf{L^4}$ respectively. The successful isolation of $\mathbf{L^{1-4}}$ was confirmed through ^1H, ^{13}C, ^{31}P NMR along with high resolution mass spectrometry. Their Eu^{3+}, Gd^{3+} and Tb^{3+} complexes were prepared using standard procedures (synthesis section ESI†). For each complex a peak corresponding to the molecular ion with the correct isotopic pattern could be observed by electrospray ionisation mass spectrometry.

Inversion recovery experiments in MOPS buffered aqueous solutions were used to determine the longitudinal relaxivities r_1 of the four complexes $\mathbf{GdL^{1-4}}$ (Table 1). The r_1 values are significantly higher than those of commercially available agents GdDTPA and GdDOTA, (4.0 and 4.2 mM^{-1} s^{-1}, respectively, at 298 K, pH 7.4, 200 MHz).[16] They are also an improvement on other recent monohydrated phosphonate appended DO3A systems.[17–20] It is important to note that most of the r_1 of the aforementioned systems have been determined at lower fields (0.47 T, 20 MHz); therefore it is likely that the difference in r_1 when compared to those of $\mathbf{GdL^{1-4}}$ will be even greater at higher magnetic fields.

The aromatic moiety also acts as an effective antenna for each of the $\mathbf{TbL^{1-4}}$ complexes. Upon excitation of the chromophore, characteristic Tb^{3+} emission bands could be observed at 489, 547, 588 and 622 nm corresponding to transitions from the $^5D_4$ to $^7F_6$, $^7F_5$, $^7F_4$ and $^7F_3$ states respectively (Fig. 2; Fig. S1–S4, ESI†). The luminescence lifetimes were measured by time-resolved measurements in H_2O and D_2O to determine

Table 1 Longitudinal relaxivities (7 T, 25 °C), luminescence lifetimes, hydration numbers and quantum yields, of $\mathbf{GdL^{1-4}}$ and $\mathbf{TbL^{1-4}}$ respectively

Complex	r_1/mM^{-1} s^{-1}, GdL	τD_2O^a/ ms	τH_2O^a/ ms	q, TbL	ΦH_2O^b, TbL
$\mathbf{LnL^1}$	7.20	3.40	2.01	0.71	0.18
$\mathbf{LnL^2}$	7.33	3.23	1.97	0.69	0.18
$\mathbf{LnL^3}$	6.65	3.10	1.90	0.72	0.27
$\mathbf{LnL^4}$	5.23	3.04	2.20	0.33	0.27

[a] Lifetimes quoted are subject to ±10% error. [b] Quantum yields determined relative to Na_3·[Tb(dpa)$_3$] in 0.1 M Tris buffer (pH 7.4) at 278 nm excitation, Φ = 0.265; estimated error ±20%.

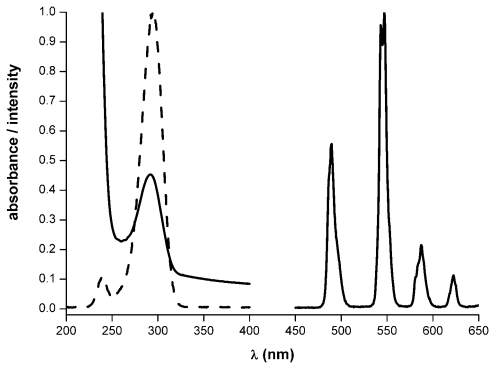

Fig. 2 Absorbance (left solid line), normalised excitation (λ_{em} 545 nm, dashed line) and emission (λ_{ex} 300 nm, right solid line) spectra of $\mathbf{TbL^1}$. The overlap of the absorbance and excitation spectra confirms that sensitised emission is occurring.

the inner sphere hydration state (Table 1).[21] $\mathbf{TbL^{1-3}}$ all have a similar q value of 0.7. When considering the available amino carboxylate donor set, this would suggest that the phosphonate group is coordinating to the metal centre. $\mathbf{TbL^4}$ has the lowest value of q at 0.3 and accordingly its Gd^{3+} analogue has the lowest r_1 value. The quantum yields (Φ) were also determined in aerated water for $\mathbf{TbL^{1-4}}$ (Table 1), ranging from 0.18 to 0.27. This demonstrates the effectiveness of the sensitised emission and the potential for these systems to be applied in optical imaging.

Sensitised emission could not be observed for the analogous $\mathbf{EuL^{1-4}}$ complexes. The excitation spectra indicated only one significant peak at 395 nm. When excited directly at this wavelength, low intensity Eu^{3+} emission bands could be observed at 580, 588, 617, 654 and 703 nm corresponding to the transitions of the $^5D_0$ excited state to the $^7F_0$, $^7F_1$, $^7F_2$, $^7F_3$ and $^7F_4$ ground levels respectively. This behaviour most likely occurs due to the quenching of the emissive state through a ligand to the metal charge transfer state.[22] Nevertheless, information about the coordination environment surrounding the Eu^{3+} can be extracted in the form of emission spectra. For each complex a distinct peak at 620 nm and a splitting of the ΔJ = 1 manifold into three components can be observed (Fig. S6–S8, ESI†). This is indicative of the phosphonate binding to the europium centre.[19,23]

Additional evidence for the interaction of the phosphonate with the Eu^{3+} centre could be provided by ^{31}P NMR spectroscopy (Fig. S9–S12, ESI†). For each of the complexes, a broad shifted peak could be observed at a range of frequencies from −75 to −116 ppm, the direction and magnitude of which have been observed previously in complexes where the phosphonate group is in close proximity to the paramagnetic center.[24]

To gain further insight into how these systems will function *in vivo*, the inversion recovery and lifetime measurements were repeated in Dulbecco's modified Eagle medium (DMEM), supplemented with fetal calf serum. This solution was designed to mimic the extracellular medium that surrounds cells *in vivo* and is used to grow cell cultures. The r_1 of the complexes $\mathbf{GdL^{1-4}}$ remained high, with only modest decreases ranging from 8 to 28% (Table S3, ESI†). Luminescence lifetime measurements in the same medium also resulted in a small increase in the lifetimes, between 1–14% (Table S4, ESI†).

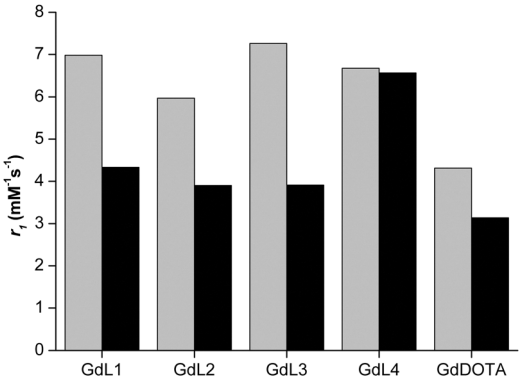

Fig. 3 Supernatant (grey) and apparent cell pellet (black) relaxivities of **GdL$^{1-4}$** and GdDOTA recorded on a 3T MRI scanner at 21 °C.

This shows that the presence of biologically important ions and amino acids does not significantly inhibit the signals arising from both types of agents.

To further examine their biocompatability, additional experiments were performed in a MRI scanner operating at 3 T (128 MHz) by mixing varying concentrations of **GdL$^{1-4}$** (20, 40, 60 and 80 μM) with 3T3 mouse fibroblasts. The T_1 values were obtained from the recorded phantom images of both the supernatant and the cell pellet. The obtained results demonstrate that the agents retain their high relaxivities in the presence of cells within the supernatant (Fig. 3). Since the exact concentration of the contrast agent in cell pellets (consisting of extracellular and intracellular volumes) is hard to assess, an apparent relaxivity $r_{1,cell}$ was determined by taking the slope of the measured relaxation rates plotted against the applied concentration. For exclusively extracellular complexes $r_{1,cell}$ should be lower than the relaxivity in solution and proportional to the reduced extracellular volume fraction since the actual concentration within the cell pellet is lower (compared to the applied concentration). As expected, there is a loss in $r_{1,cell}$ ranging from 19 to 29% for **GdL$^{1-3}$** within the cell pellet. A reduction in $r_{1,cell}$ is also observed for the extracellular agent GdDOTA to a similar extent, under the same conditions. Interestingly for **GdL^4**, such an effect was not observed. Rather, the values are almost identical, indicating that an interaction with the cells is occurring (Fig. 3). To investigate this observation, the complexes **GdL$^{1-4}$** were incubated with 3T3 cells, the supernatant was removed, the cells were washed and the T_1 values were re-measured. There is a clear enhancement of the cellular relaxation rate $R_{1,cell}$ only for **GdL^4** within the cell pellet by 22% (at 80 μM) relative to the control. Further studies would be necessary to explain whether **GdL^4** simply binds to the cell membrane or internalises into the cells.

In summary, these four ligand systems show great potential for application in bimodal imaging, satisfying many of the prerequisites required for both luminescence and MRI. They are readily prepared from cheap starting materials, employing an effective transformation to yield a multifunctional aryl phosphonate moiety. Incorporating Gd^{3+} leads to high relaxivity agents that retain their effectiveness at high magnetic fields, whilst inclusion of Tb^{3+} results in systems with long lived luminescence lifetimes and high quantum yields, suitable for use in time-gated imaging techniques. These agents are still effective when tested in more biologically relevant environments such as model extracellular medium and in the presence of cells. Moreover, two of the agents possess a phenol group which opens the possibility for further coupling reactions to other functional molecules (*e.g.* a targeting vector or an internalisation unit) which can further broaden their potential applications.

We are thankful to Dr Sven Gottschalk and Ms Hildegard Schulz, for help performing the biological experiments. Financial support of the Max-Planck Society and the German Research Foundation (DFG, grant AN 716/2-1) is gratefully acknowledged. The European COST Action D38 "Metal-Based Systems for Molecular Imaging Applications" is also acknowledged.

Notes and references

1 P. Caravan, *Chem. Soc. Rev.*, 2006, **35**, 512–523.
2 J. Yuan and G. Wang, *TrAC, Trends Anal. Chem.*, 2006, **25**, 490–500.
3 J. C. G. Bunzli, *Chem. Rev.*, 2010, **110**, 2729–2755.
4 C. P. Montgomery, B. S. Murray, E. J. New, R. Pal and D. Parker, *Acc. Chem. Res.*, 2009, **42**, 925–937.
5 L. Pellegatti, J. Zhang, B. Drahos, S. Villette, F. Suzenet, G. Guillaumet, S. Petoud and E. Toth, *Chem. Commun.*, 2008, 6591–6593.
6 A. Nonat, C. Gateau, P. H. Fries and M. Mazzanti, *Chem.–Eur. J.*, 2006, **12**, 7133–7150.
7 I. Nasso, C. Galaup, F. Havas, P. Tisnes, C. Picard, S. Laurent, L. V. Elst and R. N. Muller, *Inorg. Chem.*, 2005, **44**, 8293–8305.
8 J. E. Jones, A. J. Amoroso, I. M. Dorin, G. Parigi, B. D. Ward, N. J. Buurma and S. J. A. Pope, *Chem. Commun.*, 2011, **47**, 3374–3376.
9 C. S. Bonnet and E. Toth, *C. R. Chim.*, 2010, **13**, 700–714.
10 Z. Kotková, G. A. Pereira, K. Djanashvili, J. Kotek, J. Rudovský, P. Hermann, L. Van der Elst, R. N. Muller, C. F. G. C. Geraldes, I. Lukes and J. A. Peters, *Eur. J. Inorg. Chem.*, 2009, 119–136.
11 S. Aime, M. Botta, E. Terreno, P. L. Anelli and F. Uggeri, *Magn. Reson. Med.*, 1993, **30**, 583–591.
12 M. Botta, *Eur. J. Inorg. Chem.*, 2000, 399–407.
13 J. Rudovsky, M. Botta, P. Hermann, A. Koridze and S. Aime, *Dalton Trans.*, 2006, 2323–2333.
14 R. Frlan, S. Gobec and D. Kikelj, *Tetrahedron*, 2007, **63**, 10698–10708.
15 A. Dadabhoy, S. Faulkner and P. G. Sammes, *J. Chem. Soc., Perkin Trans. 2*, 2002, 348–357.
16 J. B. Livramento, C. Weidensteiner, M. I. M. Prata, P. R. Allegrini, C. Geraldes, L. Helm, R. Kneuer, A. E. Merbach, A. C. Santos, P. Schmidt and E. Toth, *Contrast Media Mol. Imaging*, 2006, **1**, 30–39.
17 V. Kubicek, J. Rudovsky, J. Kotek, P. Hermann, L. V. Elst, R. N. Muller, Z. I. Kolar, H. T. Wolterbeek, J. A. Peters and I. Lukes, *J. Am. Chem. Soc.*, 2005, **127**, 16477–16485.
18 P. Lebduskova, P. Hermann, L. Helm, E. Toth, J. Kotek, K. Binnemans, J. Rudovsky, I. Lukes and A. E. Merbach, *Dalton Trans.*, 2007, 493–501.
19 I. Mamedov, A. Mishra, G. Angelovski, H. A. Mayer, L. O. Palsson, D. Parker and N. K. Logothetis, *Dalton Trans.*, 2007, 5260–5267.
20 J. Rudovsky, P. Cigler, J. Kotek, P. Hermann, P. Vojtisek, I. Lukes, J. A. Peters, L. Vander Elst and R. N. Muller, *Chem.–Eur. J.*, 2005, **11**, 2373–2384.
21 A. Beeby, I. M. Clarkson, R. S. Dickins, S. Faulkner, D. Parker, L. Royle, A. S. de Sousa, J. A. G. Williams and M. Woods, *J. Chem. Soc., Perkin Trans. 2*, 1999, 493–503.
22 J. C. G. Bunzli, P. Froidevaux and J. M. Harrowfield, *Inorg. Chem.*, 1993, **32**, 3306–3311.
23 P. Atkinson, B. S. Murray and D. Parker, *Org. Biomol. Chem.*, 2006, **4**, 3166–3171.
24 J. Henig, I. Mamedov, P. Fouskova, E. Tóth, N. K. Logothetis, G. Angelovski and H. A. Mayer, *Inorg. Chem.*, 2011, **50**, 6472–6481.

